^{99m}Tc-EDDA/HYNIC-TOC and ^{18}F-FDG in thyroid cancer patients with negative ^{131}I whole-body scans

Michael Gabriel[1], Franz Froehlich[1], Clemens Decristoforo[1], Christian Ensinger[2], Eveline Donnemiller[1], Elisabeth von Guggenberg[1], Dirk Heute[1], Roy Moncayo[1]

[1] Department of Nuclear Medicine, University of Innsbruck, Innsbruck, Austria
[2] Department of Pathology, University of Innsbruck, Austria

Received: 9 August 2003 / Accepted: 1 October 2003 / Published online: 19 November 2003

Abstract. Several studies have reported on the expression of somatostatin receptors in patients with differentiated thyroid cancer (DTC). The aim of this study was to evaluate the imaging abilities of a recently developed technetium-99m labelled somatostatin analogue, ^{99m}Tc-EDDA/HYNIC-TOC (^{99m}Tc-TOC), in terms of precise localisation of disease. The study population comprised 54 patients (24 men, 30 women; age range 22–90 years) with histologically confirmed DTC who presented with recurrent or persistent disease as indicated by elevated Tg levels after initial treatment. All patients were negative on the iodine-131 post-therapy whole-body scans. Fluorine-18 fluorodeoxyglucose positron emission tomography (^{18}F-FDG PET) was performed in a subgroup of 36 patients. The study population consisted of two groups: Group A (n=22) comprised patients with disease recurrence as shown by elevated Tg levels but without detectable pathology. In group B (n=32), pre-existing lesions were known. Among the 54 cases, SSTR scintigraphy was true positive in 33 (61.1%), true negative in 4 (7.4%) and false negative in 17 (31.5%) cases, which resulted in a sensitivity of 66%. A total of 138 tumour foci were localised in 33 patients. The fraction of true positive ^{99m}Tc-TOC findings was positively correlated (P<0.01) with elevated Tg levels (higher than 30 ng/ml). Despite two false positive findings, analysis on a lesion basis demonstrated better diagnostic efficacy with ^{18}F-FDG PET (P<0.001); however, it also revealed substantial agreement between the imaging techniques [Cohen's kappa of 0.62 (0.47–0.78)]. In conclusion, scintigraphy with ^{99m}Tc-TOC might be a promising tool for treatment planning; it is easy to perform and showed sufficient accuracy for localisation diagnostics in thyroid cancer patients with recurrent or metastatic disease.

Keywords: Technetium-99m – Somatostatin – Tyrosine-octreotide – Scintigraphy – FDG-PET – Thyroid carcinoma

Eur J Nucl Med Mol Imaging (2004) 31:330–341
DOI 10.1007/s00259-003-1376-x

Michael Gabriel (✉)
Department of Nuclear Medicine,
University of Innsbruck, Anichstrasse 35,
6020 Innsbruck, Austria
e-mail: michael.gabriel@uklibk.ac.at
Tel.: +43-512-5042677, Fax: +43-512-5042683

Introduction

The overall prognosis of differentiated thyroid carcinoma (DTC) is generally rather good, with low metastatic potential and a high chance of definitive cure [1]; however, carcinoma type, stage and histological grading influence the individual outcome. Therefore, clinical surveillance after surgery and radio-ablation is very important for early detection of residual disease or recurrence. For this purpose, thyroglobulin (Tg) measurement has become a very important clinical tool. Tg determination is considered the most sensitive and specific marker of DTC [2, 3, 4]. If laboratory monitoring shows increasing Tg levels or other conventional imaging modalities are suspicious for tumour recurrence, iodine-131 (^{131}I) studies under TSH stimulation (either after withdrawal of L-thyroxine therapy or after recombinant human TSH stimulation) are required. In the event of pathological uptake, patients may undergo administration of high-dose radioiodine therapy. Importantly, detectable serum Tg levels not infrequently occur in association with negative ^{131}I whole-body scans in patients with DTC. If malignant lesions are no longer taking up radioiodine, many other techniques are used for precise localisation of malignant foci, since the treatment regimen of thyroid carcinoma patients especially depends on the size and extent of tumour when detected [5]. For localisation diagnostics at an early stage, especially if radioiodine scanning is nega-

tive, fluorine-18 fluorodeoxyglucose positron emission tomography (^{18}F-FDG PET) has already proven of value [6, 7, 8], even when other diagnostic procedures [ultrasound, computed tomography (CT), magnetic resonance imaging (MRI)] are normal. Therefore, ^{18}F-FDG PET, which characterises hypermetabolic tumour tissue, has gained widespread acceptance as a very sensitive method in the follow-up of thyroid cancer patients, although it remains an expensive procedure which is not easily available and needs adequate preparation of patients, i.e. a fasting period of at least 6 h before PET scanning. Besides ^{18}F-FDG, other unspecific oncotropic radiopharmaceuticals, e.g. ^{99m}Tc-sestamibi or ^{99m}Tc-tetrofosmin, are used for the diagnosis of recurrent and metastatic disease [9, 10, 11]. The uptake mechanism of these lipophilic cationic agents is different from that of ^{18}F-FDG, in that accumulation occurs within the mitochondria. These ^{99m}Tc-labelled tracers are advantageous in terms of availability and performance, i.e. results are independent of the blood glucose level, preparation is simple and the radiation dose is lower. However, sensitivity and specificity are moderate compared with other imaging techniques used for the follow-up of thyroid cancer [12, 13].

Another approach for localisation diagnostics is based on specific binding of radiopharmaceuticals on somatostatin receptor (SSTR)-expressing tumour lesions. SSTR scintigraphy has become a reliable, non-invasive and highly sensitive procedure for detection of a variety of endocrine and non-endocrine tumours [14, 15, 16, 17, 18].

Several studies have also reported on the expression of somatostatin receptors in DTC [19, 20, 21, 22, 23, 24, 25, 26, 27] using ^{111}In-DTPA-octreotide (Octreoscan) as the gold standard in SSTR scintigraphy. However, some results of these studies were not clearly convincing, so there is still no consensus concerning the clinical value of this technique. Taking into consideration that small and heterogeneous patient groups were investigated, i.e. several tumour types and grades showing different iodine avidity were included, the differences might have been largely related to variable and sometimes decreased density of somatostatin receptors in these tumours [28]. For our study a new ^{99m}Tc-labelled compound, ^{99m}Tc-EDDA/HYNIC-TOC (^{99m}Tc-TOC), with high SSTR-affinity, was used [29, 30]. The favourable imaging properties of ^{99m}Tc-TOC as compared with ^{111}In-DTPA-octreotide [31] makes this radiopharmaceutical a good candidate for visualisation of SSTR-expressing tumours, especially those with variable and lower receptor expression. ^{99m}Tc-TOC combines advantages of improved pharmacokinetics with higher spatial resolution due to the use of the ^{99m}Tc label. The purpose of this study was to evaluate the efficacy of the new ^{99m}Tc-labelled compound for detection of SSTR-positive lesions in a larger series of patients with recurrent or metastatic disease as shown by elevated Tg levels. All patients were negative in the post-therapy whole-body radioiodine scans. In a subset of patients we prospectively compared the SSTR profile with the metabolic pattern using ^{18}F-FDG PET in order to obtain a more complete biochemical understanding of the disease.

Materials and methods

Patient eligibility criteria. Fifty-four patients (24 men, 30 women; age range 22–90 years; mean age ± SD, 63.9±15.9 years) with histologically confirmed DTC were included for localisation diagnostics. The patients had undergone near-total thyroidectomy and radioactive ablation of the remnants and presented with either recurrent or persistent disease as indicated by elevated Tg levels. All patients showed negative results of ^{131}I post-therapy whole-body scans performed within 3 months prior to scintigraphy with ^{99m}Tc-TOC. The study population was subdivided into two groups: Group A (n=22) comprised patients with disease recurrence as shown by elevated Tg levels in serum for a minimum of two observations but without detectable pathology. Group B (n=32) consisted of patients with pre-existing lesions. Out of the 54 patients, 32 suffered from follicular, 16 from papillary and 6 from Hürthle cell carcinoma. The TNM classification according to Union Internationale Contre Cancer (UICC) [32], edition 1997, was used to classify the primary tumour. Initial pathologic tumour stages were as follows: T2 in 11 patients, T3 in 22 patients and T4 in 21 patients. The lymph node status was as follows: 21 patients were node negative (N0), 12 patients were node positive (N1a=3, and N1b=9), and 21 patients had no information concerning lymph node metastasis (Nx). Among the 54 patients, 13 initially had distant metastases (M1). The clinical staging represented the highest stage achieved during the patient's course and was determined according to the American Joint Committee on Cancer (AJCC) classification [33]; stage I was present in 5 patients, stage II in 3 patients, stage III in 4 patients to stage IV in 42 patients. Patient characteristics are given in Tables 1 and 2. The study was approved by the local ethical committee and was performed in accordance with the Declaration of Helsinki. All patients gave their written informed consent to participation.

Pretreatment evaluation and post-therapy scanning. Because of increasing serum Tg levels during TSH suppression, patients were referred to our department for administration of high-dose radioiodine therapy under TSH stimulation (in 41 patients 4 weeks after L-thyroxine withdrawal and in 13 patients after recombinant human TSH stimulation). X-ray of the chest and ultrasound of the neck were regularly performed in all patients, and CT of the chest (without contrast medium) was obtained in 24 patients. It was the second therapy for 15 patients, the third for 9, the fourth for 7, the fifth for 7, the sixth for 10, the seventh for 3 and the eighth for 3. Whole-body scans were carried out with a double-headed camera (Elscint HELIX, Haifa, Israel) 4–6 days after the therapeutic dose using a high-energy collimator. Whole-body scan results were negative.

Radiopharmaceutical. ^{99m}Tc-EDDA/HYNIC-TOC was prepared as recently described [29]. Briefly, 20 µg HYNIC-TOC was heated with 10 mg EDDA, 20 mg tricine, 15 µg stannous chloride dihydrate and 1 GBq ^{99m}Tc-pertechnetate in 2 ml 0.05 *M* phosphate buffer pH 6 at 100°C for 10 min. The solution was purified using a SepPak mini cartridge (Waters, Milford, Mass., USA) eluted with 80% ethanol and diluted with 5 ml saline. The purified radio-

Table 1. Patient characteristics and results in group A (patients without detectable pathology prior to ^{99m}Tc-TOC)

No.	Sex	Age (yrs)	Histology	TNM stage	Stage	TCD (cycles)	TSH on T_4 (mU/l)	Tg on T_4 (ng/ml)	Tg-Ab	Findings	^{99m}Tc-TOC	^{18}F-FDG	Confirmation
1	F	77	Follicular	pT3N0Mx	IV	22,747 (4)	0.3	401.2	Neg.	Lung	FN	TP	CT
2	F	70	Papillary	pT3aNxMx	IV	19,750 (4)	<0.1	32.8	Neg.	Mediastinum	FN	TP	Biopsy
3	M	22	Papillary	pT2NxMx	I	29,844 (6)	0.5	80.5	Neg.	Lymph node	FN	0	US, surgery
4	F	66	Follicular	pT2NxMx	IV	24,536 (5)	0.3	1,950	Neg.	Lung	TP	TP	CT, biopsy
5	F	75	Follicular	pT2NxMx	IV	27,780 (6)	0.6	283.3	Neg.	Mediastinum	FN	TP	Biopsy
6	M	42	Oxyphilic	pT4NxMx	II	27,280 (6)	<0.1	9.1	Neg.	Mediastinum	FN	TP	Biopsy
7	F	74	Follicular	pT3N0Mx	IV	17,552 (4)	<0.1	5.2	Neg.	Lung	FN	FN	CT
8	F	39	Papillary	pT3NxMx	I	5,631 (2)	0.3	16	Neg.	Local recurrence	FN	TP	US, surgery
9	F	77	Oxyphilic	pT2NxMx	IV	22,200 (4)	0.4	61.8	Neg.	Mediastinum	TP	TP	Surgery
10	M	44	Papillary	pT4N1bMx	IV	14,800 (3)	1.0	650	Neg.	Lymph node	TP	0	US, surgery
11	M	53	Papillary	pT3N0M0	IV	15,891 (3)	<0.1	13.4	Neg.	Lymph node	TP	TP	US, surgery
12	F	85	Follicular	pT3N1bM0	IV	29,675 (6)	<0.1	67	Neg.	Lymph node	TP	0	US, surgery
13	F	59	Follicular	pT3N0M0	IV	10,954 (2)	0.3	22.4	Neg.	Lung, mediastinum	FN	FN	CT
14	F	24	Papillary	pT4N0M0	I	9,749 (2)	<0.1	10.4	Neg.	Local recurrence	TP	0	Surgery
15	F	72	Follicular	pT3N0M0	IV	28,173 (6)	0.5	497.5	Neg.	Bone	TP	TP	MRI, SK
16	F	60	Follicular	pT4N0M0	III	11,600 (2)	0.4	9.4	Neg.	No	TN	FP	15-month FU
17	F	52	Papillary	pT4N1bMx	III	10,034 (2)	0.1	11.5	Neg.	No	TN	TN	12-month FU
18	F	90	Follicular	pT3N0M0	IV	13,657 (3)	<0.1	36.8	Neg.	Lung	FN	FN	CT
19	F	63	Follicular	pT4N0M0	III	33,906 (6)	<0.1	24.8	Neg.	Local recurrence	FN	TP	Surgery
20	F	34	Papillary	pT2NxMx	I	5,343 (2)	<0.1	7	Neg.	No	TN	FP	13-month FU
21	M	72	Oxyphilic	pT3NxMx	III	5,550 (2)	0.5	1,030	Neg.	Local recurrence, lymph node	TP	TP	Biopsy
22	F	72	Follicular	pT3NxMx	II	12,643 (3)	<0.1	13.2	Neg.	No	TN	TN	15-month FU

TNM stage, Initial tumour stage; Stage, highest tumour stage in the course of disease; TCD, total cumulative dose of ^{131}I (MBq); cycles, number of ^{131}I therapy cycles; Findings, all malignant involved tissue sites; FU, follow-up.F, Female; M, male; TCD, total cumulative dose of ^{131}I; T_4, thyroxine; Tg, thyroglobulin; TP, true positive; TN, true negative; FP, false positive; FN, false negative; FU, follow-up; SK, bone scintigraphy; other abbreviations as defined in the text

Table 2. Patient characteristics and results in group B (patients with lesions known before ^{99m}Tc-TOC)

No.	Sex	Age (yrs)	Histology	TNM stage	Stage	TCD (cycles)	TSH on T_4 (mU/l)	Tg (ng/ml)	Tg-Ab	Findings	^{99m}Tc-TOC	^{18}F-FDG	Confirmation
1	M	51	Follicular	pT3pN1bMx	IV	14,707 (3)	0.3	794	Neg.	Lung, bone	TP	TP	CT, MRI, SK
2	M	68	Follicular	pT3NxMx	IV	15,299 (3)	0.5	25.5	Neg.	Lung	FN	0	CT
3	F	70	Oxyphilic	pT4N1bM1	IV	6,550 (2)	<0.1	74	Neg.	Lung, mediastinum, lymph nodes	TP	0	US, CT, biopsy
4	M	41	Follicular	pT3N0Mx	II	12,265 (3)	1.2	1,100	Pos.	Bone	TP	TP	MRI, SK
5	F	72	Follicular	pT2N0Mx	IV	18,870 (4)	0.8	170	Pos.	Lung, mediastinum, local recurrence	TP	TP	US, CT, biopsy
6	F	77	Follicular	pT2NxMx	IV	37,261 (7)	<0.1	116	Neg.	Lung	TP	0	CT
7	F	90	Follicular	pT4N1bM0	IV	32,925 (6)	0.6	375.4	Neg.	Lung, mediastinum, local recurrence	FN	0	US, CT
8	M	82	Follicular	pT2N0M1	IV	38,200 (6)	1.1	2,700	Neg.	Lung, bone	TP	TP	CT, SK
9	M	79	Follicular	pT4N0Mx	IV	16,742 (4)	0.3	80	Neg.	Lung, local recurrence, cerebrum	TP	0	US, CT, biopsy, SK
10	M	57	Follicular	pT4NxMx	IV	20,795 (4)	<0.1	25.8	Neg.	Lung, mediastinum, bone	TP	0	CT, MRI, SK
11	M	58	Oxyphilic	pT3N1aM0	IV	12,778 (3)	0.8	1,060	Pos.	Lung, mediastinum	TP	0	CT
12	M	75	Follicular	pT4NxM1	IV	29,912 (5)	1.2	325	Neg.	Lung, bone	TP	0	CT, SK, biopsy
13	M	59	Papillary	pT4N1bM1	IV	8,595 (2)	0.9	2,062	Neg.	Lung	TP	TP	CT
14	M	68	Follicular	pT2N0M1	IV	51,000 (8)	0.3	56.6	Neg.	Lung, mediastinum, bone	TP	TP	CT, MRI, SK
15	M	46	Oxyphilic	pT4N1bM1	IV	5,699 (2)	0.3	4,490	Pos.	Lung, mediastinum	TP	0	CT, surgery
16	M	74	Papillary	pT2NxMx	IV	41,314 (7)	<0.1	209	Neg.	Lung	FN	TP	CT
17	M	64	Follicular	pT3NxM0	IV	7,104 (2)	0.6	1,300	Pos.	Bone	TP	0	MRI, SK, biopsy
18	F	74	Follicular	pT4N0M1	IV	11,955 (3)	1.3	1,020	Neg.	Bone	TP	TR	CT, SK, biopsy
19	F	87	Papillary	pT3N0M1	IV	27,750 (5)	0.7	475.4	Neg.	Lung	TP	TP	CT
20	F	81	Follicular	pT4NxM1	IV	16,873 (5)	<0.1	74	Neg.	Bone, liver	FN	0	CT, MRI, SK
21	F	75	Follicular	pT3N0M1	IV	44,979 (8)	0.4	920	Pos.	Bone	TP	0	MRI, SK
22	M	66	Papillary	pT4N1bM1	IV	26,830 (5)	1.1	4,910	Neg.	Lung	TP	TP	CT, biopsy
23	M	67	Follicular	pT3N1aMx	IV	35,672 (7)	<0.1	81.2	Neg.	Lung, mediastinum	TP	TP	CT
24	M	57	Follicular	pT2NxMx	IV	20,350 (5)	1.4	900	Neg.	Lung, mediastinum, bone	TP	TP	CT, MRI, SK, biopsy
25	F	63	Papillary	pT3N0Mx	IV	9,250 (2)	0.5	1,640	Pos.	Bone	TP	TP	CT, MRI, SK, surgery
26	F	52	Follicular	pT4N0M1	IV	44,899 (8)	0.7	154	Neg.	Bone	TP	0	CT, MRI, surgery
27	F	80	Follicular	pT4N0M1	IV	33,906 (6)	1.0	185.1	Neg.	Bone	TP	TP	MRI, SK
28	F	76	Follicular	pT3N0Mx	IV	26,241 (5)	0.2	94.3	Neg.	Lung, mediastinum	FN	0	CT, biopsy
29	M	57	Papillary	pT4NxMx	IV	12,950 (2)	1.0	429.4	Pos.	Lung, bone	TP	0	CT, MRI, SK, biopsy
30	M	38	Papillary	pT3N1aMx	I	11,100 (2)	<0.1	42.2	Neg.	Lymph node	FN	TP	US, CT, surgery
31	F	71	Follicular	pT4NxMx	IV	34,036 (6)	<0.1	630	Pos.	Lung, bone	TP	TP	CT, SK
32	M	51	Papillary	pT4NxMx	IV	9,250 (2)	<0.1	3.6	Neg.	Lung	FN	FN	CT, biopsy

TNM stage, Initial tumour stage; Stage, highest tumour stage in the course of disease; TCD, total cumulative dose of ^{131}I (MBq); cycles, number of ^{131}I therapy cycles; Findings, all malignant involved tissue sites are listed; other abbreviations as in Table 1 or the text

labelled peptide was sterilised by filtration and 350–400 MBq of the resulting solution was used for each patient study. Radiochemical purity was greater than 95% using analytical techniques based on high-performance liquid chromatography and thin-layer chromatography as described elsewhere [34].

99mTc-TOC imaging. Whole-body imaging was performed with a double-headed camera (Elscint HELIX, Haifa, Israel). For the ^{99m}Tc whole-body studies, the camera was equipped with a low-energy all-purpose parallel-hole collimator, window setting 140 keV, width 10%. For tomographic acquisition, the same double-headed gamma camera was used. Acquisition parameters were: 60 projections, 25 s/projection, matrix 64×64, zoom 1. ^{99m}Tc-TOC studies were performed 4 h p.i. and additional 2-h p.i. images were acquired if the clinical interest was related to the abdomen in order to avoid pitfalls due to unspecific bowel activity. Abdominal single-photon emission tomography (SPET) was performed in 22 patients 4 h p.i. SPET of the neck and chest was obtained in all patients and SPET of the head was obtained in 12 patients. Since many SPET acquisitions were carried out, primarily for reasons of patient convenience, given the length of the procedure, complementary scintigraphic planar images were only acquired in a small group of patients (n=14). For SPET analysis raw data were transferred to a HERMES system (Nuclear Diagnostics, London, UK) and filtered (Wiener filter) before reconstruction.

Bone scintigraphy. The same doubled-headed gamma camera as mentioned before was used for planar bone scintigraphy. Data acquisition was started 2–3 h after intravenous injection of 740 MBq ^{99m}Tc-DPD (Teceos, Schering). At least 1.5 million counts were required for each head.

18F-FDG PET. Thirty-six patients received 370 MBq (10 mCi) ^{18}F-FDG (FDG-TUM, Munich) after a fasting period of 6–12 h while still under thyroxine therapy. Between 50 and 60 min after intravenous injection of the tracer, transaxial imaging was performed using an Advance PET scanner (General Electric Medical System, Milwaukee, WI) with an axial field of view of 15.2 cm. The emission scan was acquired from the head to the upper legs with five to six bed positions, at 6 min per bed position. A transmission scan was acquired with a ^{68}Ge/^{68}Ga rod source for attenuation correction of the PET emission data, at 4 min per bed position. Iterative image reconstruction was performed with an ordered subset-expectation maximisation (OSEM) algorithm (2 iterations, 28 subsets). A visually abnormal focus of ^{18}F-FDG uptake was rated as a positive finding when the focal uptake clearly exceeded the activity profile of the surrounding tissue without connection to organs showing physiologically increased uptake and no similar activity was seen in the contralateral side of the body.

CT and MRI. Abdominal, chest and head CT scanning (Hi speed Advantage CT scanner; GE Medical System, Milwaukee, WI) was performed with 5-mm contiguous sections using a 512×512 matrix, before and after rapid i.v. infusion of contrast medium. All MR examinations were performed on a 1.5-T whole-body scanner (Magneton Vision; Siemens Medical Systems, Erlangen, Germany) by using a phased-array surface coil. T1- and T2-weighted spin-echo images were obtained with and without fat suppression. Lesions within parenchymatous organs were rated as organ metastases if they were not clearly identified as benign lesions according to standard criteria (attenuation or signal intensity and enhancement pattern after administration of contrast medium). Lymph nodes were staged morphologically according to the standard criterion of nodal diameter, i.e. lymph nodes with a diameter of more than 1 cm in the longest axis were rated as lymph node metastases. CT and/ or MRI were performed on a routine basis in all patients.

Sonography. High-resolution neck ultrasound was also performed on a routine basis using a real-time, high-frequency (7.5- to 10-MHz), small-part probe transducer. Ultrasound scanning covered the entire neck region to visualise the submandibular glands, the thyroid bed, the supra- and infraclavicular area, the superior mediastinum as far as possible and areas lateral to the carotid artery and jugular vein.

Thyroglobulin measurement. Blood samples for measuring serum Tg and anti-Tg antibody were taken prior to scintigraphy during suppression therapy. The Tg levels were determined in duplicate by a sensitive, commercially available radio-immunoassay (Brahms Dynotest Tg-S, Brahms Diagnostics, Berlin, Germany). A reference recovery value for exclusion of unspecific interactions in the serum (e.g. antibodies) was determined using the zero standard and was classified as abnormal if values >1 ng/ml were found during TSH suppression.

Image and data analysis. Somatostatin receptor images were interpreted by two nuclear medicine physicians (M.G., R.M.) blinded to the results of conventional or PET examinations. Any focal tracer accumulation exceeding normal regional tracer uptake was rated as a pathological finding (tumour uptake). Linear, non-focal limited intestinal uptake was rated as non-specific, non-pathological uptake. In relevant areas, SPET images were available to the viewer. All data were analysed on a HERMES system (Nuclear Diagnostics, London, UK). In both groups, readers of the scans were blinded to the underlying pathology and to the results of the standard staging procedures, including PET data. All images were visually evaluated and abnormal scintigraphic findings were classified according to the sites typical for recurrences or metastases (local recurrence, lymph node of the neck, mediastinum, lungs, bone structures) and other sites. The reference standard against which the results of the ^{99m}Tc-TOC procedure were measured was based on the results of all of the imaging procedures, with inclusion of serial follow-up morphological imaging and histopathology of surgical specimens or biopsy in 28 patients. All patients underwent ultrasound of the neck and imaging with either CT (n=37) or MRI (n=14), or both (n=9). Bone scanning was performed in 19 patients.

^{18}F-FDG PET was additionally performed in 18 patients of group A and 18 patients of group B. The time interval between ^{99m}Tc-TOC scintigraphy and ^{18}F-FDG PET did not exceed 4 weeks and both techniques were prospectively compared. The viewers of the studies were blinded to findings of other methods. Corresponding studies were compared for the final analysis lesion by lesion.

Statistical analysis. ^{99m}Tc-TOC images were classified as true positive, true negative, false positive or false negative by considering the gold standard (histopathology or other imaging techniques), as described above. The sensitivity, specificity and accuracy were calculated using the standard method. The sensitivity was calculated for the recognition of any lesion in the tissue belonging to five categories including local recurrence, lymph node of the neck, mediastinum, lungs and bone structures in each patient. The χ^2 test for independence, or the Fisher exact test when appropriate, was used to evaluate differences in lesion detectability with ^{99m}Tc-TOC when subgroups of the patients being investigated were sta-

tistically compared. All *P* values below 0.05 were considered to indicate statistical significance. The McNemar test of correlated properties was used to assess the statistical significance of the difference between the scintigraphic results of ^{99m}Tc-TOC and ^{18}F-FDG PET. Analysis was performed both on a lesion and on a patient basis. Two-sided *P* values less than 0.05 were considered significant. Cohen's kappa with confidence intervals of 95% was calculated to show the degree of association between the two techniques. Statistical analysis was carried out with SPSS software.

Results

Tables 1 and 2 contain a detailed summary of clinical information for each patient. Among the 54 cases, SSTR scintigraphy was true positive (TP) in 33 (61.1%), true negative (TN) in 4 (7.4%) and false negative (FN) in 17 (31.5%) cases. No false positive (FP) scan result was observed. In group A (*n*=22), which comprised patients without detectable pathology, the scan result was TP in eight, TN in four and FN in ten cases. In group B, which consisted of patients with known lesions (*n*=32), the scan result was TP in 25 patients and FN in seven patients. In three patients of this group, previously unknown lesions (two bone metastases and one pulmonary metastasis) were additionally detected with ^{99m}Tc-TOC, and later confirmed by other imaging modalities. No statistically significant difference was observed in terms of positive findings with ^{99m}Tc-TOC (*P*=0.12) when the two groups were compared. Twenty patients with follicular thyroid cancer were positive with ^{99m}Tc-TOC, as were 8 of 15 patients with papillary and five of six with Hürthle cell carcinoma. Overall, the sensitivity of ^{99m}Tc-TOC for identification of thyroid cancer was 66% on a patient basis, with a specificity of 100% and an accuracy of 68.5%. For higher stages (*n*=46), i.e. stages III and IV, sensitivity (70.4%) was higher than for stages I and II (*n*=8), in which there were only two positive scan results. Site-related findings are listed in Table 3. When ^{99m}Tc-TOC was correlated with other imaging modalities or histopathology for analysis on a lesion basis, 138 tumor foci were localised in 33 patients, affecting the following five tissues: local recurrence (*n*=5 patients), lymph node metastases in the neck (*n*=5), mediastinum (*n*=10), pulmonary metastases (*n*=19) and bone (*n*=16). In addition to a pulmonary metastasis and local tumour recurrence as assessed by biopsy, ^{99m}Tc-TOC identified a solitary brain metastasis in patient 9 of group B. In 17 patients, 46 lesions were not detected; an example was patient 21 of group B, with multiple bone and also two liver metastases of a follicular thyroid carcinoma. Only a large osteolytic metastasis in the sternum was visible. Malignancy was assessed in 28 cases by histopathology and in 38 cases by different imaging modalities: (repeated) CT (*n*=33), MRI (*n*=13), ultrasound (*n*=10) and bone scintigraphy (*n*=17). Tumour foci were confirmed by histopathology and the sum of imaging procedures in 16 cases.

^{99m}Tc-TOC and thyroglobulin

Patients were categorised into two groups in order to evaluate the influence of the current Tg level on detectability with ^{99m}Tc-TOC: those with initial serum Tg levels of <30 ng/ml (*n*=14) and those with initial serum Tg levels of >30 ng/ml (*n*=40). None of the group with Tg levels below 30 ng/ml had anti-Tg antibodies above the normal range, whereas anti-Tg antibodies were elevated in nine patients of the second group. In the group with elevated Tg levels (*n*=40), the scan result was true positive in 30 cases and false negative in seven. In the 14 patients with Tg levels lower than 30 ng/ml, scanning was negative in 11 patients, including four true negative and seven false negative results. Three cases were true positive. The fraction of true positive ^{99m}Tc-TOC findings was positively correlated with elevated Tg levels, i.e. levels higher than 30 ng/ml, showing a significant difference (*P*<0.01).

The lowest Tg level with unequivocal positive ^{99m}Tc-TOC findings was 10.4 ng/ml (patient 14 of group A, in whom local tumour growth was revealed), and the highest Tg level with false negative ^{99m}Tc-TOC scintigraphy was 401.1 ng/ml (patient 1 of group A). This patient presented with multiple pulmonary metastases, all of which were smaller than 1 cm.

^{99m}Tc-TOC and ^{18}F-FDG

True positive results were obtained in 20 patients out of 36 with ^{99m}Tc-TOC (55.5%) and in 28 patients with ^{18}F-FDG (77.7%). In 16 cases (44.4%), scintigraphy was negative with ^{99m}Tc-TOC, while ^{18}F-FDG PET was negative in six cases (16.6%). Of the 16 negative scinti-

Table 3. Scintigraphic findings: analysis per lesion

	Local recurrence	Neck (lymph node)	Mediastinum	Lung	Bone	Other	Overall
^{99m}Tc-TOC +	5	5	27	71	29	1	138
^{99m}Tc-TOC –	2	2	5	25	10	2	46
No. of lesions	7	7	32	96	39	3	184

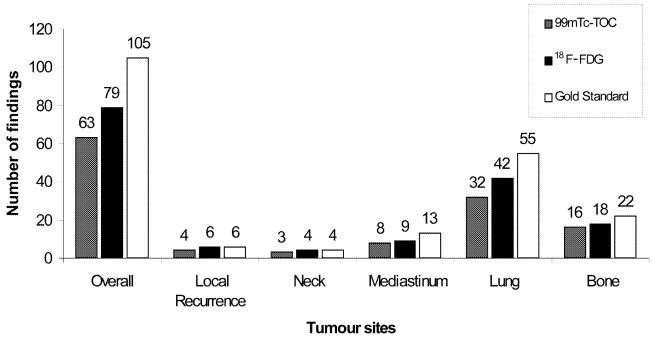

Fig 1. Number of abnormal findings revealed by ^{99m}Tc-TOC and ^{18}F-FDG PET in 36 patients and comparison with other imaging modalities and histology, i.e. the gold standard

Table 4. ^{99m}Tc-TOC and ^{18}F-FDG results

Parameter	^{99m}Tc-TOC	^{18}F-FDG
Sensitivity	62.5% (20/32)	87.5% (28/32)
Specificity	100% (4/4)	50% (2/4)
Accuracy	66.7% (24/36)	83.3% (30/36)

Number of patients is shown within parentheses

graphic studies using ^{99m}Tc-TOC in four patients (11.1%; patients 16, 17, 20 and 22 of group A), further clinical examinations did not reveal any pathological findings and serum Tg levels also remained stable over a follow-up period of at least 1 year, so these cases were considered true negative. Two of them showed suspicious uptake using ^{18}F-FDG PET, leading to false positive results. In patient 16, focal tracer accumulation was found in the right neck due to an inflammatory reaction. Asymmetrical uptake was detected in the thyroid bed in patient 20, mimicking recurrent local disease, but further cytodiagnosis confirmed granulomatous tissue. False negative scan results were obtained in 12 cases (33.3%) with ^{99m}Tc-TOC and in four cases (11.1%) with ^{18}F-FDG PET. Overall, ^{99m}Tc-TOC yielded a per-patient sensitivity of 62.5%, a specificity of 100% and an accuracy 66.7%, whereas ^{18}F-FDG showed a sensitivity of 87.5%, a specificity of 50% and an accuracy of 83.3% (Table 4). An analysis per patient comparing the scan results of ^{99m}Tc-TOC and ^{18}F-FDG showed statistically significant better results for PET (P<0.004) using the McNemar test. This correlation was based on 36 observations.

In addition, a site-specific evaluation was performed. Tissue-related abnormal uptake is reported in Fig. 1. Out of 105 malignant foci, ^{18}F-FDG PET revealed 77 tumour sites (73.3%) and ^{99m}Tc-TOC, 63 (60%). There were no false positive findings with ^{99m}Tc-TOC, whereas ^{18}F-FDG showed two false positive findings, as mentioned above. Analysis on a lesion basis also emphasised the improved diagnostic efficacy of ^{18}F-FDG PET, with a P value of <0.001. Cohen's kappa of 0.62 (0.47–0.78), however, revealed substantial agreement between the imaging techniques. The difference in detection rate was most pronounced for lung lesions: 32 of 55 lesions (58.1%) were positive with ^{99m}Tc-TOC, whereas 42 lesions were correctly identified with ^{18}F-FDG (76.3%) (Fig. 2).

Clinical impact of ^{99m}Tc-TOC

Especially in group B, a high proportion of patients showed extended tumour disease that limited the therapeutic options. Therefore, further therapeutic strategies were not significantly influenced by ^{99m}Tc-TOC findings in many cases. However, scintigraphic findings affected the further treatment decision in ten patients. Three patients were referred to external beam radiation therapy because their lesions were not amenable to surgical excision; such was the case in patient 15 of

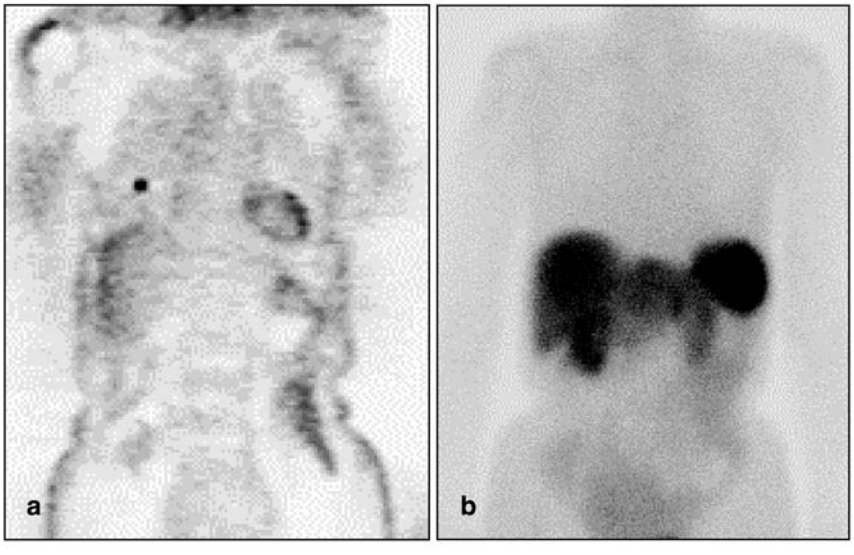

Fig 2a, b. A 77-year-old patient with follicular thyroid cancer. A solitary pulmonary metastasis, which was smaller than 1 cm, was identified with ^{18}F-FDG FDG (**a**), while ^{99m}Tc-TOC was negative (**b**)

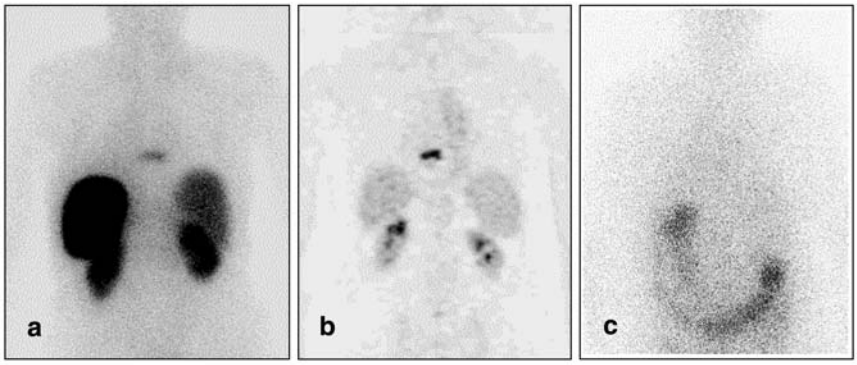

Fig 3a–c. A 72-year-old patient with follicular thyroid cancer. A matching scan result between ^{99m}Tc-TOC (**a**) and ^{18}F-FDG (**b**) was obtained for a small bone lesion in the thoracic spine, which was not depicted on the post-therapy ^{131}I whole-body scan (**c**)

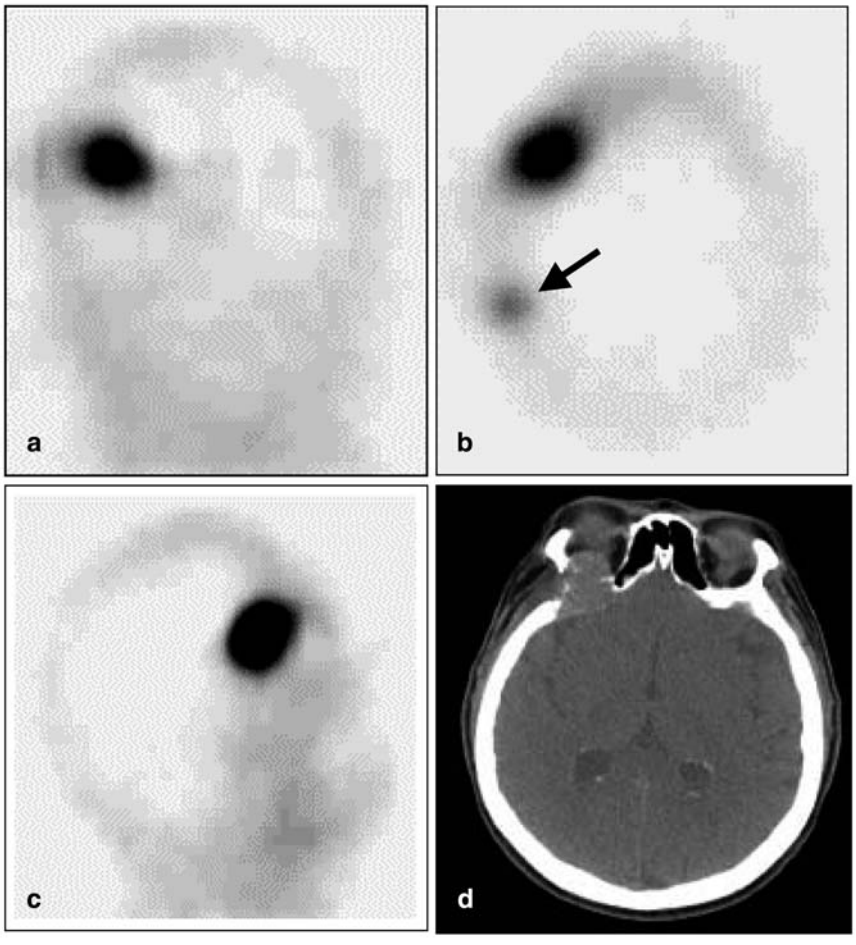

Fig 4a–d. A 52-year-old patient with follicular thyroid cancer presented with an osseous metastasis in the lateral orbital wall on the right side. This lesion was clearly delineated with SPET in the coronal (**a**), transverse (**b**) and sagittal (**c**) sections, and confirmed with CT (**d**). However, a smaller bone lesion (*arrow*) was additionally detected close to the large metastasis in the skull on the SPET acquisition (**b**), which affected further treatment planning. This patient was subsequently treated by external beam radiation, and spared surgery

group A (Fig. 3). A bone metastasis in the thoracic spine was identified with ^{99m}Tc-TOC, and also confirmed by ^{18}F-FDG. Another bone metastasis, located in the right humerus, was irradiated in patient 12 of group B. This lesion was initially described with ^{99m}Tc-TOC, whereas the other pulmonary metastases were already known before the scan. In patient 26 of group B, the intention was to remove surgically a large lesion in the lateral orbital wall. Close to this known lesion, the SPET acquisition additionally showed a smaller bone metastasis in the skull (Fig. 4), so this patient was spared from further surgical intervention and external radiotherapy was performed.

Patient 11 (Fig. 5) and patient 12 of group A showed tracer uptake in a cervical lymph node metastasis. Both patients were successfully treated by lymph node dissection, which resulted in a decrease in Tg levels without detectable pathology in the further follow-up. Only patient 21 of group A showed another increase in Tg 6 months after resection of malignant involved lymph nodes and recurrent local disease, which were initially visualised with ^{99m}Tc-TOC.

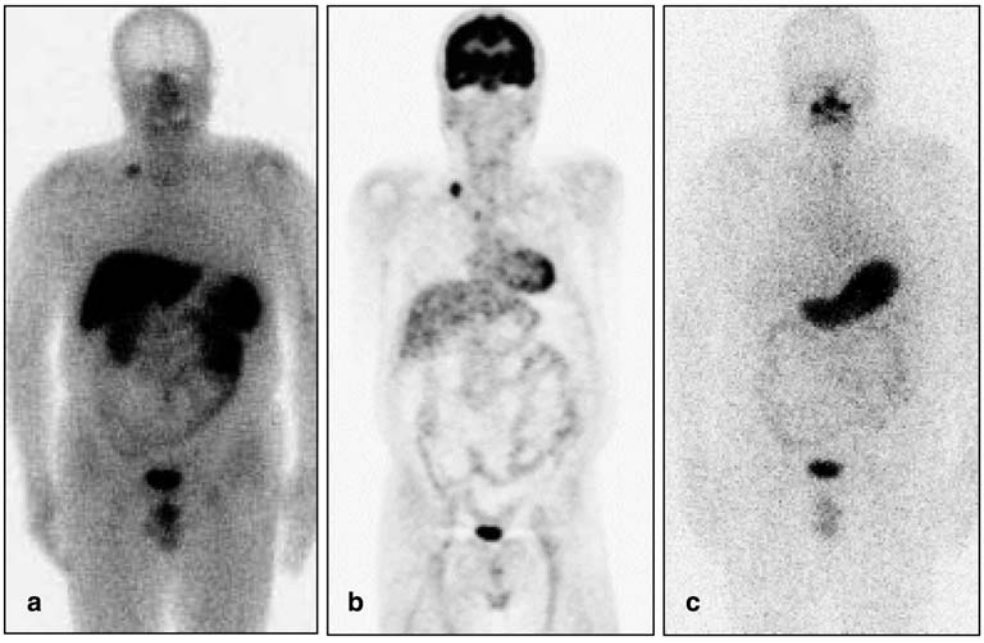

Fig. 5a–c. SSTR imaging shows a small cervical lymph node metastasis (**a**) in a patient with papillary thyroid cancer. This lesion was also intensely delineated by ^{18}F-FDG PET (**b**), but missed by post-therapy ^{131}I whole-body scan (**c**). This 53-year-old patient was successfully treated by lymph node dissection

Five patients (nos. 1, 5, 10, 13 and 25 of group B) were referred to receptor-mediated radionuclide therapy using ^{90}Y-DOTA-TOC. Intense uptake behaviour of the ^{99m}Tc-labelled radiopharmaceutical was found in several tumour lesions. All patients had extended disease with more than one affected tissue site. Each of them responded under this therapy regimen, and stable disease was achieved for at least 5 months in all patients. Each patient was well informed about this new treatment option and each of them received three or four cycles with 1,850 MBq per interval cycle. The therapy was well tolerated. In the event of tumour progression under therapy, treatment with ^{90}Y-DOTA-TOC was terminated.

Discussion

Several studies have reported on the high level of SSTR expression on various tumour cells, which provides the molecular basis for successful somatostatin receptor imaging. Despite the lack of SSTR subtype 2 in certain thyroid tumours, relatively high tumour uptake of ^{111}In-DTPA-octreotide has been observed [28]. However, the sensitivity of ^{111}In-DTPA-octreotide varies markedly among studies, which might be especially related to the variable and sometimes low expression of the receptors in DTC. Our study was performed to investigate the clinical potential of ^{99m}Tc-TOC for tumour localisation in a larger series of patients. The study was initiated because of the more favourable imaging characteristics and the higher sensitivity of this new compound as assessed by higher tumour to organ ratios, which might be based on better pharmacokinetics and the higher spatial resolution of the ^{99m}Tc label [31]. The results of the present study reflect the favourable imaging abilities of the new tracer in patients with DTC, with an overall sensitivity of 66% for detection of tumour foci in the presence of elevated Tg levels and negative radioiodine scintigraphy. The results indicate that although lesions had lost their ability to take up radioiodine, a high percentage still showed expression of SSTR. Comparing the results with those of other studies using ^{111}In-DTPA-octreotide in patients with DTC, the overall sensitivity of the present study is generally comparable or even higher [19, 20, 23, 25, 26, 27]. A limiting issue in all these studies has been the small number of patients included.

Many lesions in different body regions showed positive tracer uptake, i.e. 138 of 184 lesions were detected in 33 patients, with higher probability for a positive scan result in patients with higher Tg levels exceeding 30 ng/ml, which might be mainly attributed to the tumour load. However, the spatial resolution of the ^{99m}Tc-labelled compound is insufficient to detect smaller lesions, e.g. in the presence of widespread pulmonary metastases. In our series of patients, 25 of 96 lung lesions escaped detection, and in these cases the lesion diameter was usually less than 1 cm. Although tumour load and Tg levels were sometimes high in these cases, the scan result was inconclusive, as exemplified in Fig. 6. The patient with the highest Tg level with false negative ^{99m}Tc-TOC scintigraphy (patient 1 of group A) also presented with multiple pulmonary metastases, all of which were smaller than 1 cm.

When comparing ^{99m}Tc-TOC and ^{18}F-FDG, a pronounced difference was also found concerning the rate of detection of pulmonary metastases, which was 58.1% and 76.3% respectively. One explanation might be the higher spatial resolution of PET. However, a biological

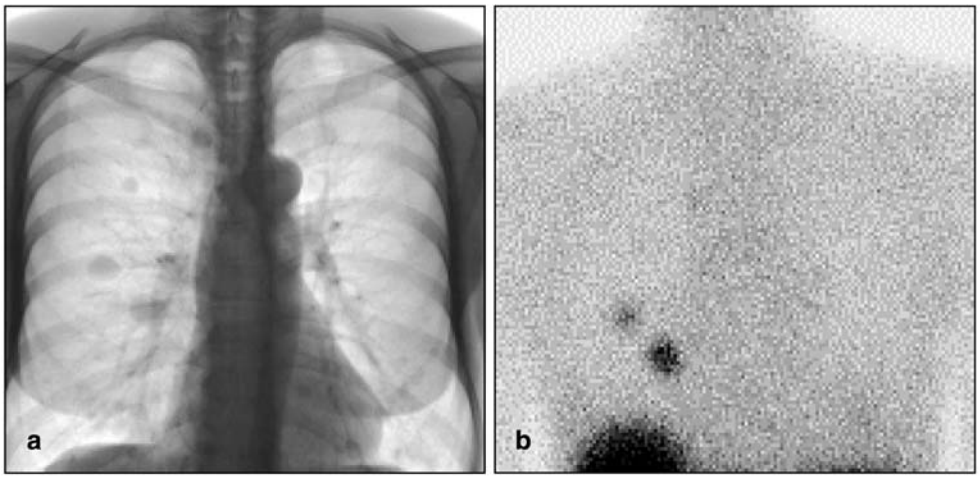

Fig. 6a, b. This 77-year-old patient with a serum Tg of 116 ng/ml suffered from multiple pulmonary metastasis of a follicular thyroid carcinoma, as shown in the chest X-ray (**a**). Positive ^{99m}Tc-TOC uptake was only found in the two largest lesions in the right lung (**b**)

phenomenon cannot be excluded, which could imply that some hypermetabolic lesions do not express SSTR. In paragangliomas and carcinoid tumours, Le Rest et al. showed that the different mechanism of uptake resulted in variation in tumour affinity for ^{111}In-DTPA-octreotide compared with ^{18}F-FDG, i.e. Octreoscan identified some lesions which were negative with ^{18}F-FDG PET and vice versa [35].

In the 36 patients of the present study who underwent ^{18}F-FDG PET, the diagnostic efficacy was statistically significantly higher for ^{18}F-FDG PET than for ^{99m}Tc-TOC, although two false positive findings on ^{18}F-FDG PET were negative on ^{99m}Tc-TOC. However, there was substantial overlap in the lesions detected by each modality, which implies high agreement between the metabolic pattern and the SSTR status in non-iodine-avid lesions. From the clinical point of view, both techniques can easily be performed without withdrawal of L-thyroxine, as long as some precautions are taken in the case of PET, e.g. a 6-h fasting period before scanning. Although there is no evidence that serum TSH levels influence the rate of somatostatin receptor expression, higher glucose consumption in tumour foci can be observed under TSH stimulation, which could improve the accuracy of ^{18}F-FDG PET [36]. In accordance with the prospective design of the present study, all investigations were performed under TSH suppression.

High ^{18}F-FDG uptake suggests more aggressive tumour cell growth in those types of lesion which have lost the sodium-iodine symporter activity. In such cases, it is highly doubtful whether high-dose radioiodine therapy will have an impact on the tumour growth [37]. If such lesions are not accessible to surgical treatment, e.g. localised disease, only a few non-invasive treatment options are available, with a low impact on the individual prognosis. Recently, it was reported that the metabolic activity as assessed by ^{18}F-FDG PET decreased in tumour lesions after the use of a long-acting octreotide analogue in patients with metastatic thyroid cancer that exhibited somatostatin receptors [38]. This new approach, with the aim of inhibiting the proliferation of neoplastic tissue, seems very promising considering the benefit of somatostatin analogues in patients suffering from other SSTR-expressing malignancies, e.g. neuro-endocrine tumours of the gastroenteropancreatic system [39]. Long-acting somatostatin analogues can also be used in multimorbid patients, e.g. elderly patients with reduced kidney function.

High expression of somatostatin receptors in thyroid carcinoma lesions also offers another treatment option using radionuclide targeted therapy, e.g. ^{90}Y-DOTA-TOC [40]. We have followed this rationale in five patients with advanced tumour stage who had a very high tumour load. These patients showed intense tumour uptake of ^{99m}Tc-TOC. Prior to the use of either ^{90}Y-labelled or unlabelled long-acting derivatives, the assessment of SSTR status in tumour lesions seems mandatory. In different clinical settings, somatostatin receptor imaging with ^{99m}Tc-TOC easily allows non-invasive selection of the subset of patients who would benefit from such therapies.

In the case of DTC, ^{99m}Tc-sestamibi is currently a preferred radiopharmaceutical. ^{99m}Tc-sestamibi, however, exhibits only a moderate detection rate with respect to lymph node metastases [41]. By contrast, we found that ^{99m}Tc-TOC provided high spatial resolution in the neck, given that five of seven sites in the neck corresponding to lymph node metastases and also five of seven cases of local tumour recurrences were correctly identified. Beside accurate anatomical localisation to permit adequate treatment planning, ^{99m}Tc-TOC could help in the development of new surgical techniques, e.g. probes for minimally invasive radio-guided surgery, avoiding extensive surgery in the neck. A similar approach has been taken with ^{99m}Tc-sestamibi in a small series of patients with recurrent thyroid cancer [42], but there is as yet no evidence whether this technique is accurate enough to detect malignant involved cervical lymph nodes. Since the

mechanism of uptake of the lipophilic cationic agent is different from that of ^{99m}Tc-TOC, further investigations are needed to evaluate which of the two ^{99m}Tc-labelled compounds is better in terms of localisation diagnostics and treatment stratification in patients with recurrent or metastatic disease.

In conclusion, somatostatin receptor imaging using ^{99m}Tc-TOC is a promising and easy-to-perform technique for accurate anatomical localisation of malignant foci in thyroid cancer patients with elevated Tg levels and negative ^{131}I scans. Although ^{18}F-FDG showed a higher sensitivity in our series of patients, with the advent of new therapeutic approaches, e.g. minimally invasive radio-guided surgery or application of SST analogues, this new technique might be an effective tool to improve treatment strategies in DTC.

Acknowledgements. We especially wish to thank Prof. G. Riccabona, Prof. Emeritus, University of Innsbruck, for his help and support in initiating this study.

References

1. Pacini F, DeGroot LJ. Thyroid neoplasia. In: DeGroot LJ, Jameson JL, eds. *Endocrinology, 4th edn.* Philadelphia: Saunders; 2001:1541–1566.
2. Ronga G, Fiorentino A, Paserio E, et al. Can iodine-131 whole-body scan be replaced by thyroglobulin measurement in the post surgical follow-up of differentiated thyroid carcinoma. *J Nucl Med* 1990; 31:1766–1771.
3. Ozata M, Suzuki S, Miyamoto T, Tsuan Liu RT, Fierro-Renoy F, Degroot LJ. Serum thyroglobulin in the follow-up of patients with treated differentiated thyroid cancer. *J Clin Endocrinol Metab* 1994; 79:98–105.
4. Lubin E, Mechli-Frish S, Zatz S, et al. Serum thyroglobulin and iodine-131 whole-body scan in the diagnosis and assessment of treatment for metastatic differentiated thyroid carcinoma. *J Nucl Med* 1994; 35:257–262.
5. Schlumberger MJ. Diagnostic follow-up of well-differentiated thyroid carcinoma: historical perspective and current status. *J Endocrinol Invest* 1999; 22 (11 Suppl):3–7.
6. Feine U, Lietzenmayer R, Hanke JP, Held J, Woehrle H, Mueller-Schauenburg W. Fluorine-18-FDG and iodine-131-iodide uptake in thyroid cancer. *J Nucl Med* 1996; 37:1468–1472.
7. Schlueter B, Bohuslavizki KH, Beyer W, Plotkin M, Buchert R, Clausen M. Impact of FDG PET on patients with differentiated thyroid cancer who present with elevated thyroglobulin and negative^{131}I scan. *J Nucl Med* 2001; 42:71–76.
8. Helal BO, Merlet P, Toubert ME, et al. Clinical impact of ^{18}F-FDG PET in thyroid carcinoma patients with elevated thyroglobulin levels and negative ^{131}I scanning results after therapy. *J Nucl Med* 2001; 42:1464–1469.
9. Briele B, Hotze A, Kroopp J, et al. A comparison of ^{201}Tl and ^{99m}Tc-MIBI in the follow-up of differentiated thyroid carcinomas. *Nuklearmedizin* 1991; 30:115–124.
10. Lind P, Gallowitsch HJ, Langsteger W, Kresnik E, Mikosch P, Gomez I. Technetium-99m-tetrofosmin whole-body scintigraphy in the follow-up of differentiated thyroid carcinoma. *J Nucl Med* 1997; 38:348–354.
11. Miyamoto S, Kasagi K, Misaki T, Alam MS, Konishi J. Evaluation of technetium-99m-MIBI scintigraphy in metastatic differentiated thyroid carcinoma. *J Nucl Med* 1997; 38:352–356.
12. Rubello D, Mazzarotte R, Casara D. The role of technetium-99m methoxyisobutylisonitrile scintigraphy in the planning of therapy and follow-up of patients with differentiated thyroid carcinoma after surgery. *Eur J Nucl Med* 2000; 27:431–440.
13. Ng DCE, Sundram FX, Sin AE. ^{99m}Tc-sestamibi and ^{131}I whole-body scintigraphy and initial serum thyroglobulin in the management of differentiated thyroid carcinoma. *J Nucl Med* 2000; 41:631–635.
14. Krenning EP, Kwekkeboom DJ, Bakker WH, et al. Somatostatin receptor scintigraphy with [111-In-DTPA-D-Phe] and [123-I-Tyr]-octreotide: the Rotterdam experience with more than 1000 patients. *Eur J Nucl Med* 1993; 20:716–731.
15. Krenning EP, Kwekkeboom DJ, de Jong M, et al. Essentials of peptide receptor scintigraphy with emphasis on somatostatin analog octreotide. *Semin Oncol* 1994; 21 (Suppl 13):6–14.
16. Lamberts SWJ, Reubi JC, Krenning EP. Somatostatin and the concept of peptide receptor scintigraphy in oncology. *Semin Oncol* 1994; 21 (Suppl) 13:1–5.
17. Kwekkeboom D, Krenning EP, de Jong M. Peptide receptor imaging and therapy. *J Nucl Med* 2000; 41:1704–1713.
18. Balon HR, Goldsmith SJ, Siegel BA, et al. Procedure guidelines for somatostatin receptor scintigraphy with ^{111}In-pentetreotide. *J Nucl Med* 2001; 42:1134–1138.
19. Tenenbaum F, Lumbroso J, Schlumberger M, Caillou B, Fragu P, Parmentier C. Radiolabeled somatostatin analog scintigraphy in differentiated thyroid carcinoma. *J Nucl Med* 1995; 36:807–810.
20. Baudin E, Schlumberger M, Lumbroso J, Travagli JP, Caillou B, Parmentier C. Octreotide scintigraphy in patients with differentiated thyroid carcinoma: contribution for patients with negative radioidine scan. *J Clin Endocrinol Metab* 1996; 81:2541–2544.
21. Ahlman H, Tisell LE, Wangberg B, et al. The relevance of somatostatin receptors in thyroid neoplasia. *Yale J Biol Med* 1997; 70:523–533.
22. Gulec SA, Serafini AN, Sridhar KS, et al. Somatostatin receptor expression in Hürthle cell cancer of the thyroid. *J Nucl Med* 1998; 39:243–245.
23. Garin E, Devillers A, Le Cloirec J, et al. Use of indium-111 pentetreotide somatostatin receptor scintigraphy to detect recurrent thyroid carcinoma in patients without detectable iodine uptake. *Eur J Nucl Med* 1998; 25:687–694.
24. Kolby L, Wangberg B, Ahlman H, et al. Somatostatin receptor subtypes, octreotide scintigraphy, and clinical response to octreotide treatment in patients with neuroendocrine tumors. *World J Surg* 1998; 22:679–683.
25. Valli N, Catargi B, Ronci N, et al. Evaluation of indium-111 pentetreotide somatostatin receptor scintigraphy to detect recurrent thyroid carcinoma in patients with negative radioiodine scintigraphy. *Thyroid* 1999; 9:583–589.
26. Haslinghuis LM, Krenning EP, De Herder WW, Reijs AE, Kwekkeboom DJ. Somatostatin receptor scintigraphy in the follow-up of patients with differentiated thyroid cancer. *J Endocrinol Invest* 2001; 24:415–422.
27. Goerges R, Kahaly G, Mueller-Brand J, Maecke H, Roser HW, Bockisch A. Radionuclide-labeled somatostatin analogues for diagnostic and therapeutic purposes in nonmedullary thyroid cancer. *Thyroid* 2001; 11:647–659.

28. Forssell-Aronsson EB, Nilsson O, Benjegard A, et al. ^{111}In-DTPA-D-Phe^{1}-octreotide binding and somatostatin receptor subtypes in thyroid tumors. *J Nucl Med* 2000; 41:636–642.
29. Decristoforo C, Melendez-Alafort L, Sosabowski JK, Mather SJ. ^{99m}Tc-HYNIC-[Tyr3]-octreotide for imaging somatostatin-receptor-positive tumors: preclinical evaluation and comparison with ^{111}In-octreotide. *J Nucl Med* 2000; 41:1114–1119.
30. Decristoforo C, Mather SJ, Cholewinski W, Donnemiller E, Riccabona G, Moncayo R. ^{99m}Tc-EDDA/HYNIC-TOC: a new ^{99m}Tc-labelled radiopharmaceutical for imaging somatostatin receptor-positive tumours: first clinical results and intra-patient comparison with ^{111}In-labelled octreotide derivates. *Eur J Nucl Med* 2000; 27:1318–1325.
31. Gabriel M, Decristoforo C, Donnemiller E, et al. An intrapatient comparison of ^{99m}Tc-EDDA/HYNIC-TOC with ^{111}In-DTPA-octreotide for diagnosis of somatostatin receptor expressing tumors. *J Nucl Med* 2003; 44:708–716.
32. Sobin LH, Wittekind C. International Union Against Cancer. *TNM classification of malignant tumours, 5th edn.* New York: Wiley-Liss, 1997.
33. American Joint Committee on Cancer. *AJCC cancer staging manual, 5th edn.* In: Part II: 8. Thyroid Gland. Philadelphia, New York: Lippincott-Raven; 1997:59–61.
34. Decristoforo C, Mather SJ. Preparation, ^{99m}Tc-labelling and in vitro characterisation of HYNIC and N_3S modified RC-160 and [Tyr^{3}]-octreotide. *Bioconjug Chem* 1999; 10:431–438.
35. Le Rest C, Bomanji JB, Costa DC, Townsend CE, Visvikis D, Ell PJ. Functional imaging of malignant paragangliomas and carcinoid tumours. *Eur J Nucl Med* 2001; 28:478–482.
36. Petrich T, Boerner AR, Otto D, Hofmann M, Knapp WH. Influence of rhTSH on [^{18}F]fluorodeoxyglucose uptake by differentiated thyroid carcinoma. *Eur J Nucl Med Mol Imaging* 2002; 29:641–647.
37. Wang W, Larson SM, Tuttle RM, et al. Resistance of [^{18}F]-fluorodeoxyglucose-avid metastatic thyroid cancer lesions to treatment with high-dose radioactive iodine. *Thyroid* 2001; 11:1169–1175.
38. Robbins RJ, Hill RH, Wang W, Macapinlac HH, Larson SM. Inhibition of metabolic activity in papillary thyroid carcinoma by a somatostatin analogue. *Thyroid* 2000; 10:177–183.
39. Arnold R, Simon B, Wied M. Treatment of neuroendocrine GEP tumours with somatostatin analogues: a review. *Digestion* 2000; 62 Suppl 1:84–91.
40. Waldherr C, Schumacher T, Pless M, et al. Radiopeptide transmitted internal irradiation of non-iodophil thyroid cancer and conventionally untreatable medullary thyroid cancer using [^{90}Y]-DOTA-D-Phe^{1}-Tyr^{3}-octreotide: a pilot study. *Nucl Med Commun* 2001; 22:673–678.
41. Hsu CH, Liu FY, Yen RF, Kao CH. Tc-99m MIBI SPECT in detecting metastatic papillary thyroid carcinoma in patients with elevated human serum thyroglobulin levels but negative I-131 whole body scan. *Endocr Res* 2003; 29:9–15.
42. Rubello D, Piotto A, Pagetta C, Pelizzo MR, Casara D. ^{99m}Tc-MIBI radio-guided surgery for recurrent thyroid carcinoma: technical feasibility and procedure, and preliminary clinical results. *Eur J Nucl Med Mol Imaging* 2002; 29: 1201–1205.